

## Electronic Supplementary Information

# **Anisotropic Wettability Manipulation via Capturing Architected Liquid Bridge Shapes**

Ji Hoon Kim,<sup>a</sup> Jaekyoung Kim,<sup>b</sup> Sohyun Kim,<sup>c</sup> Hyunsik Yoon<sup>b,c,\*</sup> and Won Bo Lee<sup>a,\*</sup>

<sup>a</sup> Department of Chemical and Biological Engineering, Seoul National University, Seoul 08826, Republic of Korea

<sup>b</sup> Department of New Energy Engineering, Seoul National University of Science and Technology, Seoul, 01811, Republic of Korea

<sup>c</sup> Department of Chemical and Biomolecular Engineering, Seoul National University of Science and Technology, Seoul, 01811, Republic of Korea

**\*Corresponding authors.** E-mail: [wblee@snu.ac.kr](mailto:wblee@snu.ac.kr); [hsyoon@seoultech.ac.kr](mailto:hsyoon@seoultech.ac.kr)

## Contents :

### 1. Extended experimental methods

1.1 Fabrication of the master mold and stamp .....	4
1.2 The direct transfer of viscous pre-polymer droplets on the protruding stamp .....	4
1.3 Fabrication of the substrates with elastomeric spacer .....	5
1.4 Fabrication of derivatives of LBSM .....	5

### 2. Calculations

2.1 Geometry of liquid bridge .....	7
2.2 Calculation of initial volume .....	9
2.3 Estimated values of apparent contact angles on the LBSM .....	10

### 3. Supplementary Tables

<b>Table S1.</b> The estimated value of apparent contact angle ( $\theta^*$ ) on the transferred LBSM. The values in parentheses are experimental values .....	11
<b>Table S2.</b> The estimated value of apparent contact angle ( $\theta^*$ ) on the adhered LBSM. The values in parentheses are experimental values .....	11
<b>Table S3.</b> Overview of fabrication techniques for re-entrant structures.....	12

### 4. Supplementary Figures

<b>Fig. S1.</b> The direct transfer of photocurable polymer droplets .....	13
<b>Fig. S2.</b> Consecutive LBSM images according to adhesion force differences and liquid bridge height. $H_{crit}$ was denoted to classify the “R” region and “ $\theta$ ” region .....	14
<b>Fig. S3.</b> Fracture of LBSM in the detaching process by applied stress .....	15
<b>Fig. S4.</b> Scheme and Images of LBSM with prism-shaped tips.....	16
<b>Fig. S5.</b> Scheme of LBSM fabrication using a negative stamp .....	17
<b>Fig. S6.</b> SEM images of adhered SU-8 LBSMs with stamps made of various polymers .....	18

**Fig. S7.** Measurement of the advancing ( $\theta_{adv}$ ) and receding ( $\theta_{rec}$ ) contact angle of water on the LBSMs consisting of SU-8,PDMS and PUA .....19

**Fig. S8.** SEM image to calculate solid fraction of LBSM .....20

**Fig. S9.** Cross-sectional view of experiments on directional liquid manipulation.....21

**Fig. S10.** Statistical calculation of the initial volume of liquid droplets using image analysis .22

**Fig. S11.** Chemical structures of monomers, oligomers, and photoinitiators (PI) .....23

**5. Supplementary Movies**

**Movie S1.** Isotropic/anisotropic wettability manipulation through LBSMs .....24

**Movie S2.** Measurement of dynamic contact angle of water on the SU-8 LBSMs.....24

**Movie S3.** Measurement of dynamic contact angle of water on the PDMS LBSMs.....24

**Movie S4.** Measurement of dynamic contact angle of water on the PUA LBSMs.....24

**References** .....24

## **1. Extended experimental methods**

### **1.1 Fabrication of the master mold and stamp**

We fabricated a master mold with SU-8 (Kayaku, Microchem) on a silicon wafer using photolithography. An elastomeric negative mold was fabricated by pouring a PDMS (Sylgard 184, Dow corning) elastomer base mixed with a curing agent (10:1 weight ratio) over the master mold in a Petri dish, and then baking it for 4h at 65°C. Continuously, the protruding pillar stamp was fabricated via soft lithography. Cut glass slides (size: 26mm \* 26mm \* 1mm) were employed as a supporting backplane for regular pattern formation over a large area. To enhance adhesion of the glass and the stamp, we applied oxygen plasma (CUTE, Femtoscience, 100W, 50sccm) for 60s and put them on a vacuum chamber ( $\sim 10^{-2}$  torr) for 1hr to deposit TMSPMA in vapor phase before soft lithography.

### **1.2 The direct transfer of viscous pre-polymer droplets on the protruding stamp**

SU-8 precursor mixed with acetone (1:1 weight ratio) was spin-coated on a cover glass (at 2000rpm, for 30s). And then the stamp was placed on a spin-coated precursor film. We slightly pressed the mold for about 10s and detached the mold. After transferring pre-polymer droplets on the stamp, the stabilization time was taken for about 10min until the droplets have the equilibrium shape.

### **1.3 Fabrication of the substrates with elastomeric spacer**

In the case of polymer substrates, a prepolymer thin film was spin-coated on a glass substrate and exposed to UV to be cured (Heat was applied in the case of thermocurable polymer). We employed cut glass slides (size: 26mm \* 26mm \* 1mm) as a supporting backplane.

We put a cut PET film (size: 20mm \* 30mm \* 50 $\mu$ m) on the center of the cut glass slide and attached adhesive tapes to fix the PET film. And then we prepared mixture of PDMS elastomer base and curing agent (or the mixture of this with acetone solvent, 1:1 weight ratio). This mixture was spin-coated on the substrate with PET film from 1000rpm to 4000rpm and then baking it for 4h 65°C. After hardening the elastomeric film, we detached the adhesive tapes and pulled out the PET film. Height of the spacer was adjusted by controlling the spin coating condition. In the case of the elastomeric spacer with a lower modulus, we employed Ecoflex rubber (the mixture of part A and part B, 1:1 weight ratio).

### **1.4 Fabrication of derivatives of LBSM**

#### a) Substrate derivatives

We first prepared a curved PDMS substrate through the following process. Rectangular-shaped PET film was fixed bent over a Petri dish. In the case of a 2D curved structure, we fixed two PET films biaxially. And we poured PDMS oligomer (10:1 weight ratio) and was cured for 4h at 65°C. To fabricate wrinkled LBSM, PUA oligomer was spin-coated on a glass substrate and exposed to UV for 1min to form a partially cured film mediated by oxygen inhibition. Then we deposited thin Au film (~5nm) using a sputtering device (SPT-20, COXEM Co., Ltd.) to form a micro-sized wrinkle on the surface. Additional UV was applied to the backplane of the substrate to enhance

adhesion between metal and polymer surfaces. In the case of a nanostripped pattern, we prepared a PUA pattern using soft lithography from a Si master mold. Then we poured PDMS oligomer (10:1 weight ratio) and was cured for 4h at 65°C to fabricate a patterned PDMS substrate.

b) Stamp derivatives

A line patterned stamp and negative pyramidal stamp were prepared using soft lithography from a Si master mold. Acrylate with relatively high surface energy (PUA 301) was employed as a stamp material to form integrated half-cylindrical line features, instead of PFPE. On the other hand, droplets must be isolated through Discontinuous Dewetting (DD), PDMS was employed as a stamp material. Discontinuous Dewetting (DD) was employed through the doctor blading technique. In the case of hierarchical structure, we prepared an adhered LBSM stamp through double-replication from the original LBSM pattern.

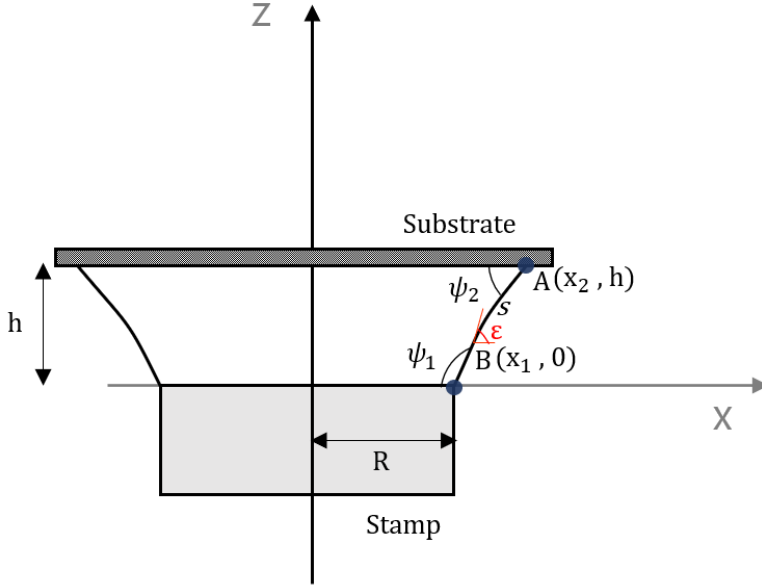
c) Compositions

PDMS oligomer solution mixed with toluene, thiol-ene oligomer mixed with acetone, and PEGDA mixed with acetone were used as solutions for spin-coating (1:1, 2:1, 1:1 weight ratio respectively). To verify the fact that it can be transferred to various materials, glass, PEGDA, and Au substrates respectively utilized as the representative of Ceramics, Polymer, and Metal.

## 2. Calculations

### 2.1 Geometry of liquid bridge

To investigate geometry of the liquid bridge between pillars and a substrate, we employed cartesian coordinate system.



A geometric relation of the liquid bridge with arc length  $s$  as a independent variable is governed by

$$\frac{dx}{ds} = -\cos(\epsilon) \quad (S1)$$

$$\frac{dz}{ds} = \sin(\epsilon) \quad (S2)$$

Where  $\epsilon$  is the angle between the curve and horizontal axis, and  $s$  is the arc length of the liquid bridge. And two radius of curvature  $R_1$ ,  $R_2$  can be expressed as

$$R_1 = \frac{x}{\sin(\epsilon)}, R_2 = \frac{ds}{d\epsilon} \quad (S3)$$

Then we can obtain mean curvature  $H$  from the definition

$$H = 0.5 \left( \frac{1}{R_1} + \frac{1}{R_2} \right) \quad (\text{S4})$$

If (1), (2), (3), and (4) are all combined, an integrated governing equation (Equation 6 in the main text) can be derived

$$2H = \frac{\frac{dz}{dx}}{x \left[ 1 + \left( \frac{dz}{dx} \right)^2 \right]^{1/2}} + \frac{\frac{d^2z}{dx^2}}{\left[ 1 + \left( \frac{dz}{dx} \right)^2 \right]^{3/2}} \quad (\text{S5})$$

To obtain an analytical solution, this equation can be further simplified with more manipulation.<sup>[1]</sup>

Using (S1) and (S2), geometric relations can be expressed as

$$\frac{dz}{dx} = -\tan(\varepsilon) = \frac{\sin(\varepsilon)}{\sqrt{1 - \sin^2(\varepsilon)}} > 0 \quad (\text{S6})$$

where  $\varepsilon \in (0, \pi)$ . Using (S3) and (S4),  $H$  can be rewritten with as  $2H = -u/x - du/dx$  ( $u \equiv \sin(\varepsilon)$ )

and

$$x = x(\varepsilon) = \frac{\sin \varepsilon \pm \sqrt{\sin^2 \varepsilon - 4Hc}}{2H} \quad (\text{S7})$$

where  $c$  is an integration constant. For a concave bridge, the "-" sign is chosen. Meanwhile, for a convex bridge, the "+" sign is chosen. There are two boundary conditions at points A and B:

$$\text{At point A, } x=x_1, \varepsilon = \pi - \psi_1 \quad (\text{S8})$$

$$\text{At point B, } x=x_2, \varepsilon = \pi - \psi_2 \quad (\text{S9})$$

Integration constant  $c_A, c_B$  can be calculated using (S7), (S8), and (S9). All integration constants must be equal,  $c = c_A = c_B$ , then  $H$  can be expressed as

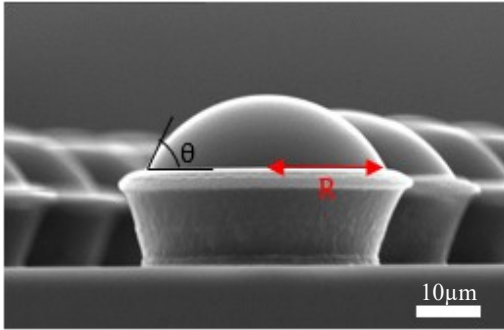
$$H = \frac{x_1 \sin(\psi_1) - x_2 \sin(\psi_2)}{x_1^2 - x_2^2} \quad (\text{S10})$$

Then, Laplace pressure can be obtained from the definition of the Young-Laplace equation

$$\Delta P = 2H\gamma_{LV} = 2\gamma_{LV} \frac{x_1 \sin(\psi_1) - x_2 \sin(\psi_2)}{x_1^2 - x_2^2} \quad (\text{S11})$$

There is no inflection point (just exists undulation point) in the profile, so we used the second-order function for describing the curve:  $x(z) = az^2 + bz + c$ . Therefore, liquid bridge profile can be calculated by applying boundary conditions according to each state.

## 2.2 Calculation of initial volume



Initial volume of a liquid droplet can be calculated from the following equation.

$$V_0 = \pi * \frac{R^3}{\sin(\theta)} * \left( \frac{2}{3} - \cos\theta + \frac{\cos^3\theta}{3} \right) \quad (\text{S12})$$

$\theta$  was measured from SEM images and  $R$  was calculated statistically using image analysis (Figure S7).

### 2.3 Estimated values of apparent contact angles on the LBSM

#### 1) Transferred LBSM

In the case of transferred LBSM, surface is chemically heterogeneous, therefore Cassie-Baxter relation <sup>[2]</sup> can be applied. If  $\theta_E < \psi$ , a liquid droplet meets all composite surface, therefore  $\theta^*$  can be calculated by

$$\cos(\theta^*) = f_1 \cos(\theta_{E,1}) + f_2 \cos(\theta_{E,2}) \quad (\text{S13})$$

where  $f_1$  and  $f_2$  are the fractional surface areas occupied by LBSM and the substrate ( $f_1 + f_2 = 1$ ), and  $\theta_{E,1}$  and  $\theta_{E,2}$  are equilibrium contact angles on SU-8 and substrate. If  $\theta_2 < \psi$ , air pocket is trapped below the re-entrant structure, and  $\theta_{E,2}$  becomes  $\pi$ , therefore  $\theta^*$  can be expressed as

$$\cos(\theta^*) = -1 + f_1 \{ \cos(\theta_{E,1}) + 1 \} \quad (\text{S14})$$

#### 2) Adhered LBSM

In the case of  $\theta_E > \psi$ ,  $\theta^*$  can be calculated by (S14), because it satisfies Cassie state.<sup>[2]</sup>

However, if  $\theta_E < \psi$ ,  $\theta^*$  can be estimated by Wenzel's relation, because adhered LBSMs are chemically homogeneous structure made by double replica molding. Therefore,  $\theta^*$  can be calculated by

$$\cos(\theta^*) = r \cos(\theta_E) \quad (\text{S15})$$

where  $r$  is roughness of the surface. Since  $r$  is not bounded, if RHS becomes bigger than 1, the surface can be totally wetted unlike with chemically heterogeneous cases. The parameters required to calculate  $\theta^*(r, \theta_E \text{ and } f_1)$  were measured from the SEM images and contact angle meter.

### 3. Supplementary Tables

	'R' region	'theta' region	
Water	72.6 (74.3)	156.4(150.0)	■ Estimated by (S13) ■ Estimated by (S14)
Olive oil	37.1 (38.1)	151.4(145.3)	
Hexadecane	33.5 (35.5)	46.8(48.1)	

**Table S1.** The estimated value of apparent contact angle ( $\theta^*$ ) on the transferred LBSM. The values in parentheses are experimental values.

	NOA 81	PUA 301	PEGDA	PFPE
water	156.9 (163.4)	149.6 (152.5)	150.1 (152.0)	156.9 (166.8)
Olive oil	143.4 (142.9)	145.2 (146.6)	144.0 (144.9)	145.7 (150.9)
Hexadecane	~0 (0)	~0 (0)	~0 (0)	145.1 (148.54)

■ Estimated by (S14)  
■ Estimated by (S15)

**Table S2.** The estimated value of apparent contact angle ( $\theta^*$ ) on the adhered LBSM. The values in parentheses are experimental values.

Method	Description	Advantages	Disadvantages
Replica molding with selective etching	Photolithography followed by selective etching	Effective, reliable, reproducible, durable, and optically transparent surfaces	Polymer-based materials are susceptible to harsh conditions or forces, difficulties in peeling-off step as the structures can be damaged, complex, and costly etching procedure
Replica molding without selective etching	Using a stack of bilayer photosensitive polymers or double-step UV exposures	Simple, rapid, and consistent, no need for complicated etching step	Polymer-based materials are susceptible to harsh conditions or forces, difficulties in peeling-off step as the structures can be damaged
Template molding	Pre-forming vertical pillars by injection molding or hot embossing process and then fabricating the wide mushroom tips	Simple, inexpensive, better control of the tip size and shape, intact surface without deformation due to peeling-off, suitable for high aspect ratio	Lack of uniformity in lateral shape and spatial length
Silicon micromachining	Removing silicon materials by wet chemical or dry plasma processes	Ideal method for fabrication doubly re-entrant structures	Very complicated and time-consuming multi-step procedure, require high expertise handling
Direct laser writing	Two-photon polymerization-based 3D printing	Precise, flexible, and rapid, can form complex arbitrary structures	Low throughput and low control in terms of tailoring large-area samples
Electroplating	Electrodepositing material onto a master pattern	Well-controlled tip size and shape	Low control of microstructure growth location
Bottom-up	Growing randomly-distributed re-entrant structures on a substrate	Simple, suitable for large scale production	Disordered distribution, low surface roughness
Electrospinning	Producing microfibers or nanofibers with re-entrant structures	Simple, suitable for large scale production	Inhomogeneous fiber distribution, low robustness against wetting
Ours* (included in template molding method)	Sculpting and solidifying liquid bridges between micropillars and a substrate	Simple, cost-effective, facile controllability of size and shape and versatility in morphologies and compositions	Limitation of scale by the size of the mold and requirement of highly viscous liquid for high aspect ratio structures

**Table S3.** Summary of re-entrant fabrication methods (reprinted from reference [3] with minor revisions)

## 4. Supplementary Figures

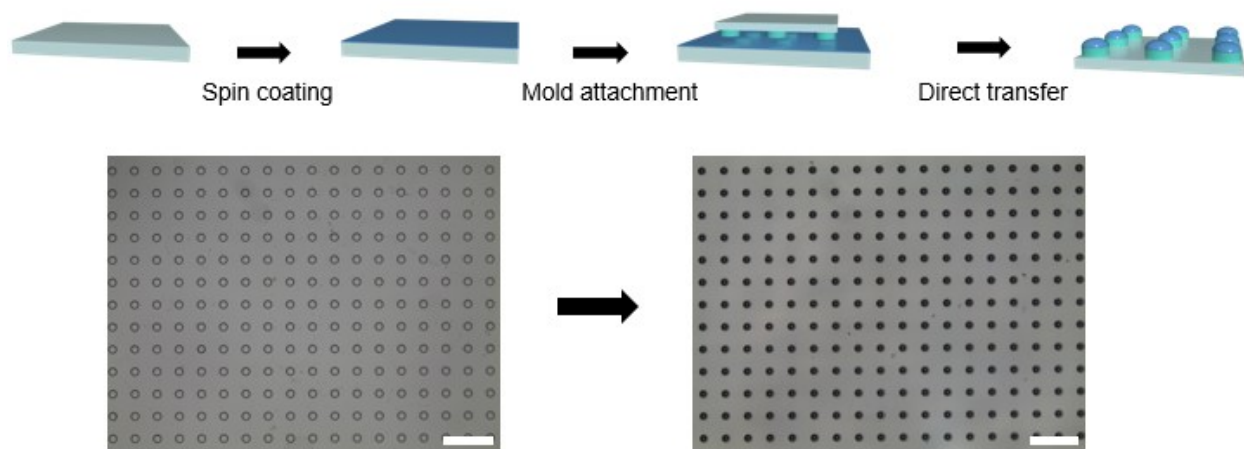


**Figure S1.** The direct transfer of photocurable polymer droplets. All scale bars represent 100 μm.

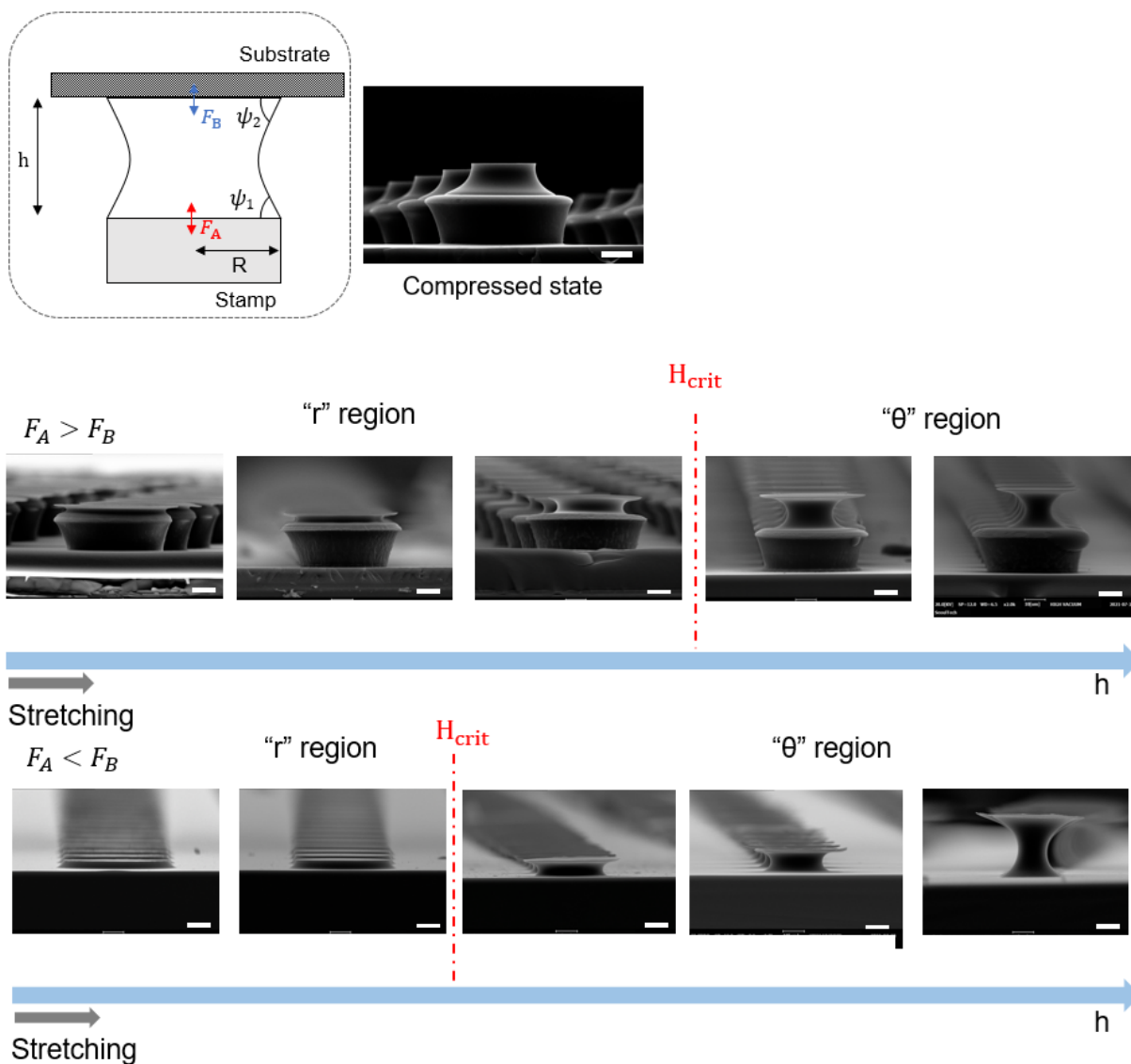


**Figure S2.** Consecutive LBSM images according to adhesion force differences and liquid bridge height.  $H_{crit}$  was denoted to classify the “r” region and “θ” region. All scale bars represent  $10\mu\text{m}$ .

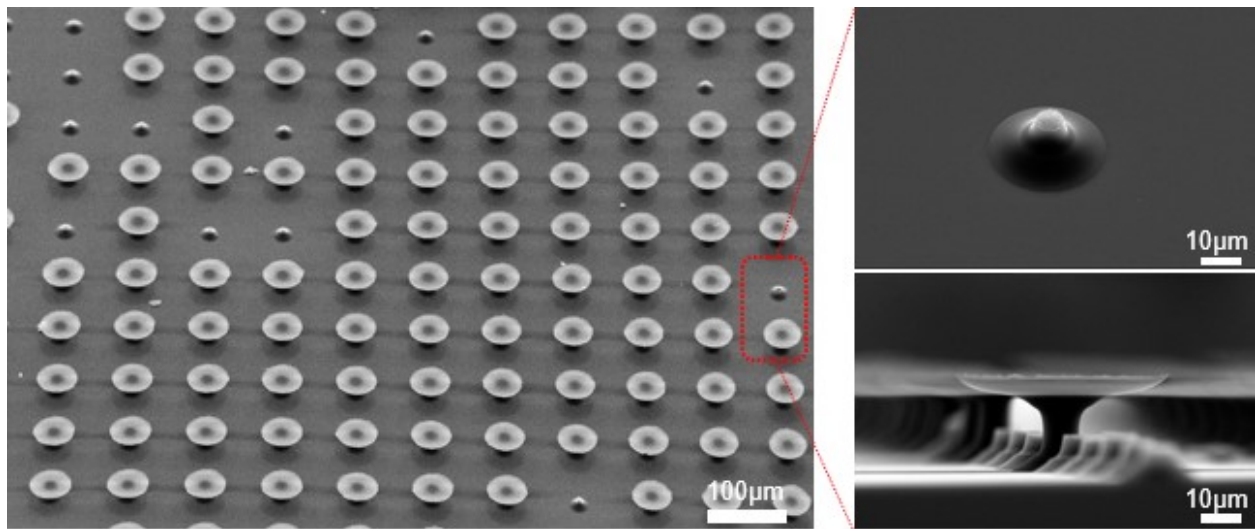


**Figure S3.** Fracture of LBSM in the detaching process by applied stress.

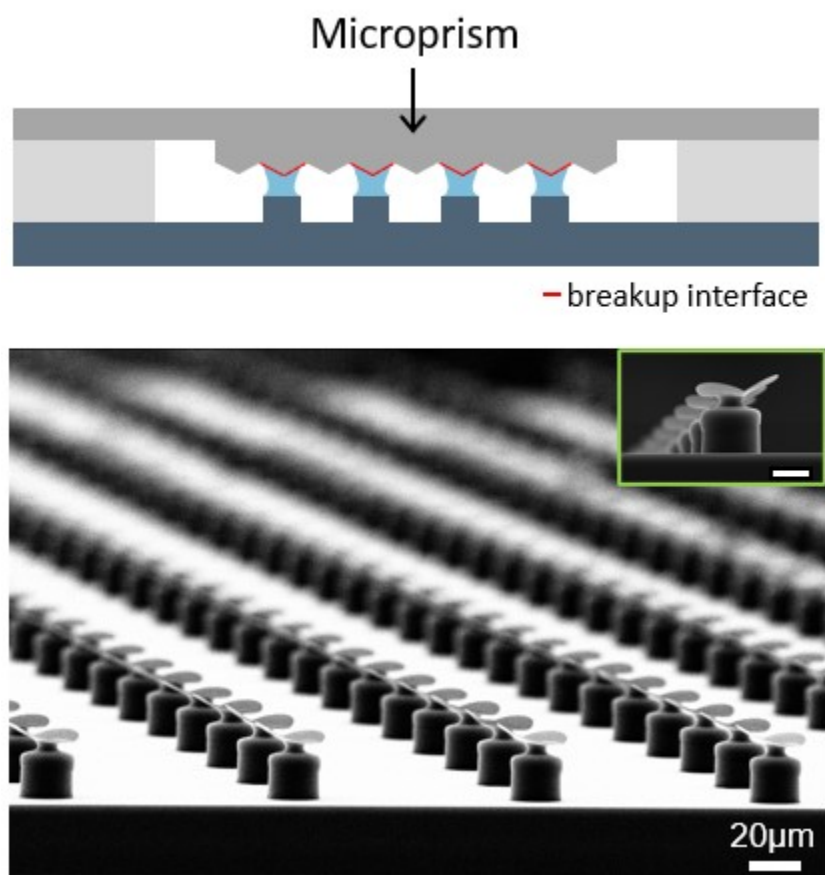


**Fig. S4.** Scheme and Images of LBSM with prism-shaped tips. The scale bar of the inset image represents 10 $\mu$ m.

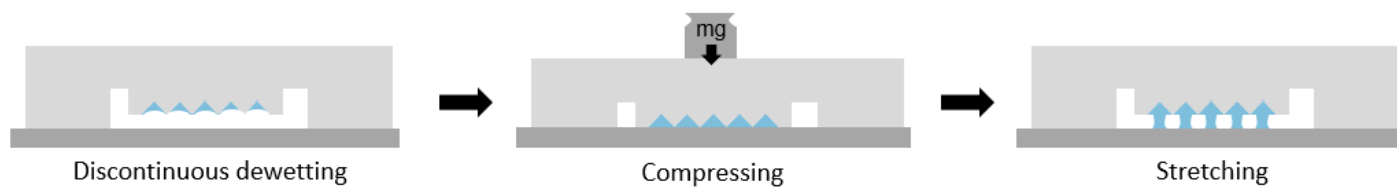


**Figure S5.** Scheme of LBSM fabrication using a negative stamp. Discontinuous dewetting (DD) was employed to form discontinuous liquid droplets on the engraved elastomeric stamp.

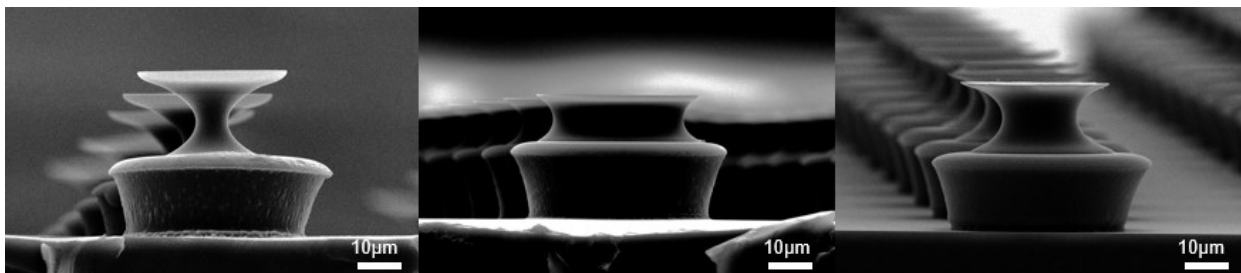


**Figure S6.** SEM images of adhered SU-8 LBSMs with stamps made of PEGDA, PUA, and thiol-ene (NOA81).

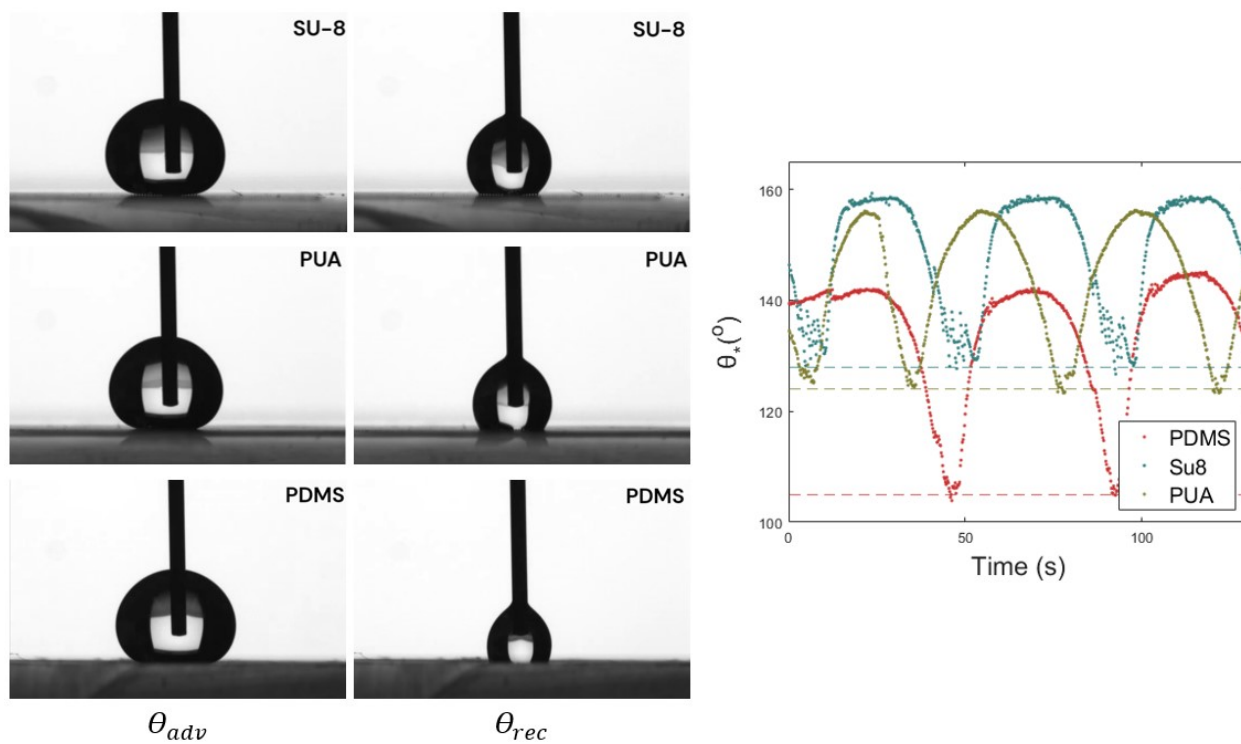


**Figure S7.** Measurement of the advancing ( $\theta_{adv}$ ) and receding ( $\theta_{rec}$ ) contact angle of water on the LBSMs consisting of SU-8, PUA and PDMS.

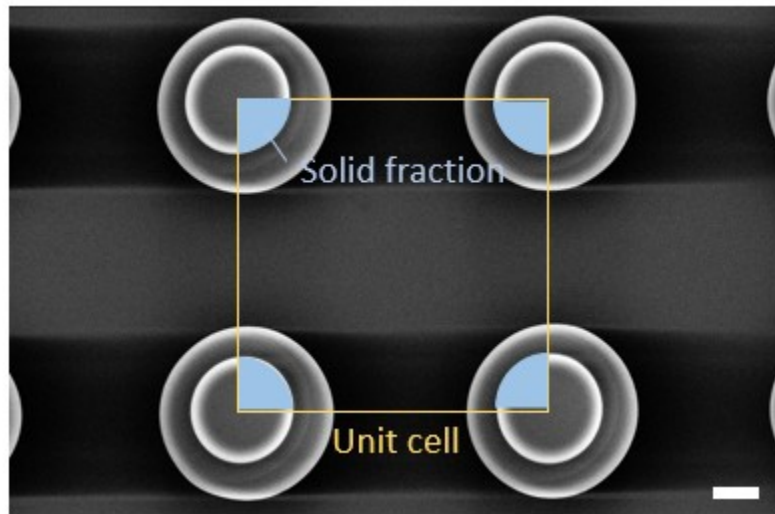


**Figure S8.** SEM image to calculate solid fraction of LBSM. The scale bar represents 10 $\mu$ m.

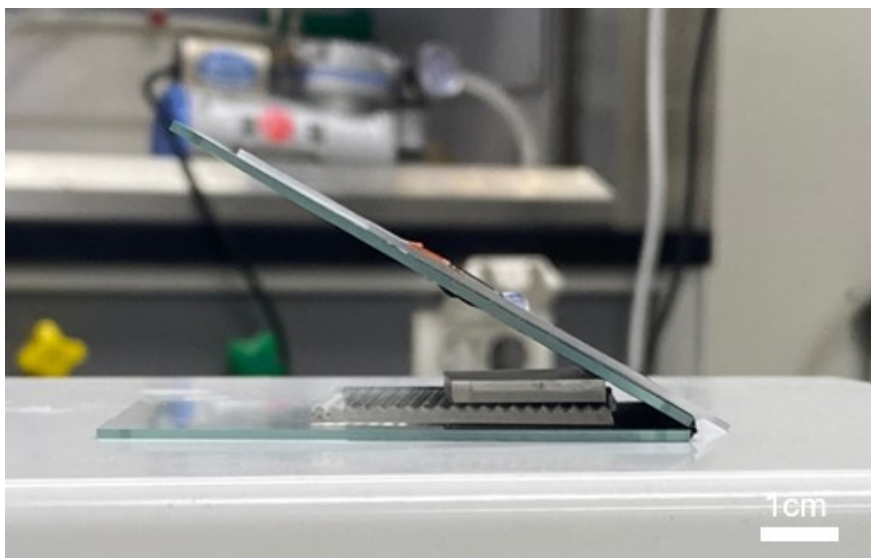


**Figure S9.** Cross-sectional view of experiments on directional liquid manipulation. The sliding experiment was conducted on  $29^\circ$ .

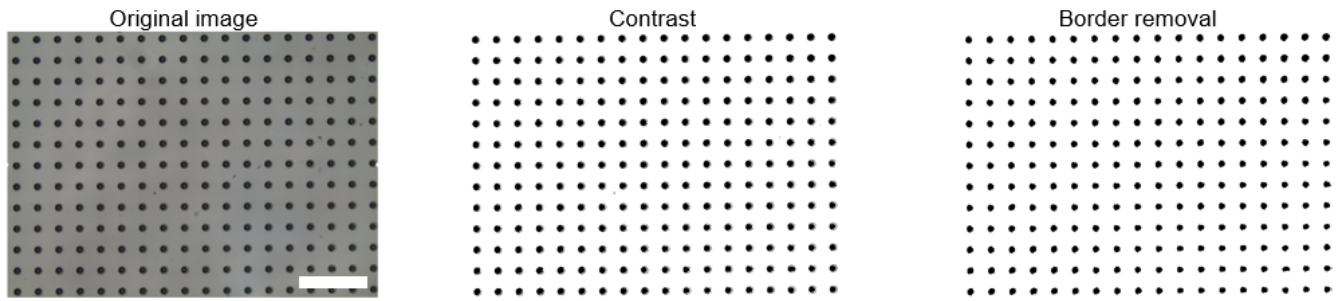


**Figure S10.** Statistical calculation of the initial volume of liquid droplets using image analysis. We employed the contrast enhancement method and binarization for removing the border and getting liquid droplets in black only. Moreover, we utilized a circle detection tool to calculate an average radius of the pillars. The scale bar represents 100 $\mu\text{m}$ .



## 5. Supplementary Movies

**Movie S1.** Anisotropic wettability manipulation through LBSMs. A droplet with high surface energy ( $\gamma \sim 72.6$  mN/m) rolled down the tilted direction. A droplet with moderate surface energy ( $\gamma \sim 42.9$  mN/m) experienced rolling to flowing transition. In the case of low surface energy ( $\gamma \sim 21.9$  mN/m), the droplet directly flowed along the perpendicular lines.

**Movie S2.** Measurement of dynamic contact angle of water on the LBSMs made of SU-8 (2cycles).

**Movie S3.** Measurement of dynamic contact angle of water on the LBSMs made of PDMS (2cycles).

**Movie S4.** Measurement of dynamic contact angle of water on the LBSMs made of PUA (2cycles).

## References

- 1 Y. Wang, S. Michielsen and H. J. Lee, *Langmuir*, 2013, 29, 11028-11037.
- 2 P.-G. d. Gennes, *Capillarity and wetting phenomena: drops, bubbles, pearls, waves*, Springer, New York, 2004.
- 3 H. H. Vu, N. T. Nguyen, N. Kashaninejad, *Adv. Mater. Tech.*, 2023, 2201836.